Nanoscale Systems for Optical Quantum Technologies

Grant Agreement No: 712721
Start Date: 1st October 2016 - Duration: 36 months

D1.7 Coherence in Er^{3+} nanostructures

Deliverable:	D1.7
Work package:	WP1 Nano-materials, optical micro-cavities and control systems
Task:	1.1 Y2O3 nanoparticles development
Lead beneficiary:	ICFO-QP
Type:	Report
Dissemination level:	Public
Due date:	30 September 2019
Actual submission date:	30 September 2019
Author(s):	Bernardo Casabone, Hugues de Riedmatten (ICFO-QP), Diana Serrano, Philippe Goldner (CNRS-CP)

This project has received funding from the European Union's Horizon 2020 research and innovation programme under grant agreement No 712721.

Version history

Version	Date	Author(s)	Description
V1	19.09.2019	Bernardo Casabone, Hugues de Riedmatten (ICFO)	First Draft
V2	23.09.2019	Inputs from P. Goldner and D. Serrano (CNRS-CP)	Final version submitted to EU

Table of Contents

Deliverable Description

This deliverable describes our measurements to infer spectroscopic properties of erbium doped nanostructures, such as optical coherence, inhomogeneous broadening of the $^4I_{15/2}$-$^4I_{13/2}$ optical transition and population lifetime of the excited state. We first show measurements at room temperature performed on Er^{3+}: Y_2O_3 nanoparticle powder, where we measure the optical linewidth and the optical lifetime. We then present measurements performed at low temperature in a closed-cycle cryostat. We measured the inhomogeneous linewidth, the optical lifetime and the homogenous linewidth of Er^{3+}: Y_2O_3 ceramics. We performed two-pulse photon echo measurements as a function of temperature, between 2.7 and 5 K, revealing homogeneous linewidth as low as 200 kHz at 2.7 K, and of 800 kHz at 5 K. Finally, we investigated a promising alternative system for realizing spin-photon interfaces, Pr^{3+}: Y_2O_3 nanoparticles. We measured the optical and spin coherence properties of nanoparticles of different sizes. We measured optical and spin coherence times of up to 3 and 800 µs, respectively.

Er^{3+}:Y_2O_3: Room temperature spectroscopy

Before performing experiments at cryogenic temperature, we have performed room temperature characterization of the optical line and lifetime of Er^{3+} doped nanocrystals.

Our samples are 200 ppm Er^{3+}: Y_2O_3 nanocrystals synthesized by CNRS-CP following the methods described in D1.2 and 1.4. The average crystal diameter is 150 nm. Measurements in this section were performed using a macroscopic ensemble of nanocrystals in the form of a powder. To perform the measurements, the powder was placed in a holder, and resonant spectroscopy was obtained around 1535 nm. In order to obtain the data, we performed pulsed excitation and detection for which we used an InGaAs avalanche photodiode (APD). For the measurement of the linewidth, we scanned the frequency of the excitation laser, and we recorded the fluorescence emitted by the nanoparticles as a function of the excitation wavelength. Fig. 1 shows the optical linewidth and the lifetime obtained at the center of the line. We measured an optical linewidth of 130 GHz. At this temperature, it is likely that this linewidth mostly corresponds to the homogeneous linewidth. The population lifetime was measured to be 13.3 ms. The lifetime in the nanoparticles is longer than the one measured in the ceramic at low temperature (see next section). This difference is attributed to the smaller index of refraction seen by the nanoparticles [1].

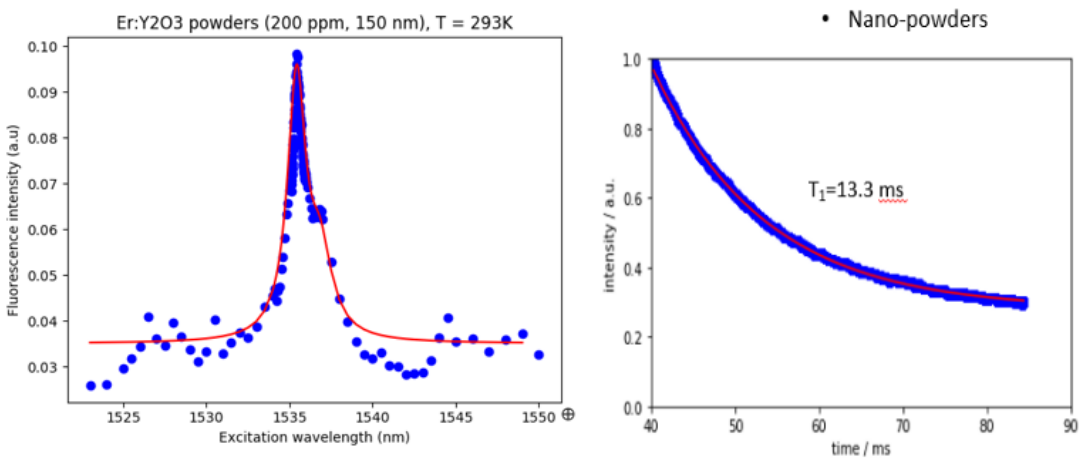

Figure 1: (left) optical inhomogeneous linewidth of the $^4I_{15/2}$-$^4I_{13/2}$ transition (right) optical lifetime obtained at the center of the line.

Er^{3+}:Y_2O_3: Low temperature spectroscopy

Characterization of Er^{3+}: Y_2O_3 thin ceramics

This section presents the results of the measurements of the inhomogeneous linewidth γ_{inhomo}, of the optical lifetime T_1 and of the homogeneous linewidth γ_{homo} of the $^4I_{15/2}$-$^4I_{13/2}$ transition in Er^{3+}: Y_2O_3 ceramics. We measured samples with various Er concentration (200 ppm, 0.2 %, 0.5 % and 1 %) and with a thickness of 300 µm. The samples were fabricated by CNRS-CP using solid-state reactions at high temperatures and measured at ICFO-QP. We used a small magnetic field, i.e. 20 Gauss, and temperatures ranging from 2.7 to 5 K. Spectral hole burning experiments were unsuccessful, probably due to the low magnetic field. The measurements were taken using a closed-cycle cold-finger cryostat.

Inhomogeneous linewidth:

The inhomogeneous linewidth was extracted both by fluorescence and from absorption measurements. For the former, the fluorescence was coupled to an optical fiber and detected with a single photon counter as a function of the excitation wavelength. For the

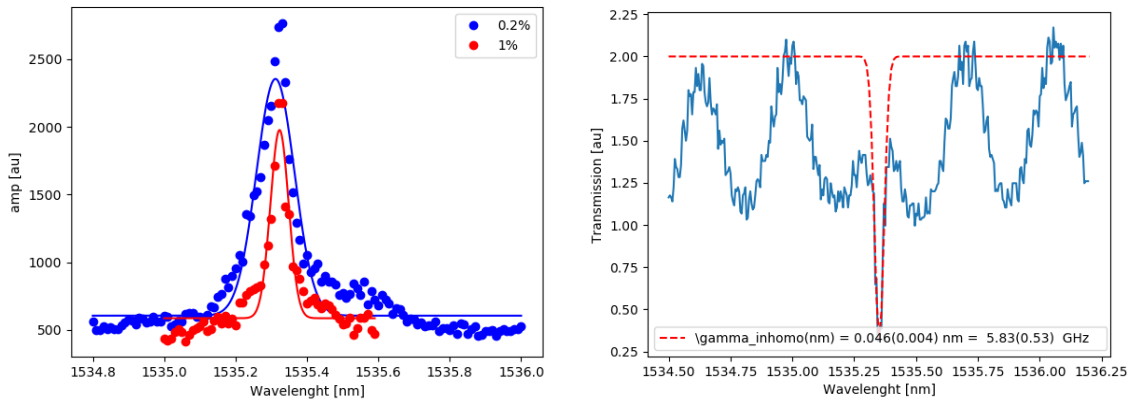

***Figure 2**: (left) excitation spectrum measured by fluorescence for the 0.2% and 1% concentration samples (right) absorption spectrum of a 200 ppm, 300 µm thick Er:Y_2O_3 ceramic at 2.7 K.*

latter, the transmitted intensity was measured as a function of the wavelength using CW light and detected using an APD. Fig. 2 shows excitation spectra for the 0.2 % and 1 % samples, and the absorption spectrum for the sample with 200 ppm Er concentration.

In Fig. 2 right, the plot shows a dip at around 1535.35 nm with FWHM of 0.046(4) nm, which corresponds to an inhomogeneous linewidth $\gamma_{inhomo} = 5.8(5)$ GHz. The oscillation of the transmission around the resonance is attributed to interference due to reflections on the uncoated windows of the cryostat. The measured linewidth for 0.2% and 1% doped samples was 8 and 4 GHz respectively. From the comparison, one can conclude that the linewidth does not strongly depend on the doping concentration.

Lifetime measurements:

To measure the optical lifetime T_1 at low temperature, we send a short and intense pulse at 1535.35 nm to the sample. The scattered fluorescence is measured using an APD. Once the pulse if off, a very weak exponential tail can be seen, which corresponds to the spontaneous emission of the erbium ions. Then, the lifetime is extracted by an exponential fit to the decay.

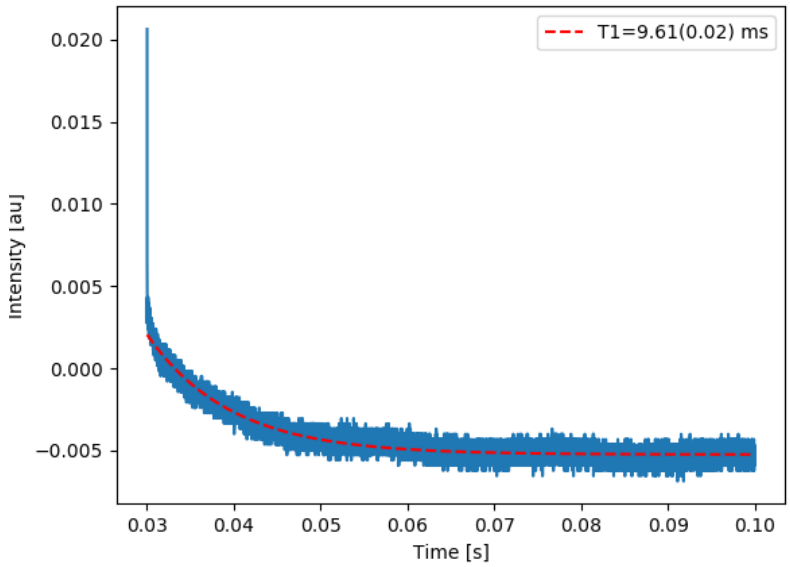

***Figure 3**: Optical lifetime T_1 measurement of a 200 ppm Er^{3+}:Y_2O_3 ceramic.*

As seen from the plot, the lifetime T_1 is measured to be 9.61(0.02) ms. Previous samples at 0.2% and 1% doping concentration showed similar results, indicating negligible concentration quenching.

Homogeneous linewidth

We then performed two-pulse photon echo experiments to assess the optical coherence lifetime of the Er^{3+} doped material. The homogenous linewidth was extracted from the decay of the two-pulse photon echo as a function of the storage time $t_{storage}$;

$$I_{echo} \propto I_0 \, e^{-4t_{12}/T_2}$$

where $t_{12} = t_{storage}/2$ is the time between the $\pi/2$- and the π - pulses and $T_2 = \frac{1}{\pi \gamma_{homo}}$

where γ_{homo} is the homogeneous linewidth. The echo intensity I_{echo} was measured using the heterodyne detection technique, i.e. by mixing the emitted echo with a local oscillator detuned by 12 MHz.

We could not observe any echo for highly doped samples, i.e. between 0.2% and 1%. However, we could observe echoes for a sample with a doping concentration of 200 ppm. We took data between 2.7 K and 6 K for a magnetic field close to 20 Gauss. The π /2- and π -pulses were 200 ns long. The waiting time between the π /2- and the π - pulses were varied between 50 and 2000 ns. We tried shorter π /2- and π -pulses but the echo was almost not visible.

Fig. 4 shows the plots of the I_{echo} vs $t_{storage} = 2 *$ (200 ns + waiting time) for 2.7 and 5K. At a temperature of 2.7 K, we find T_2 =1.6 µs.

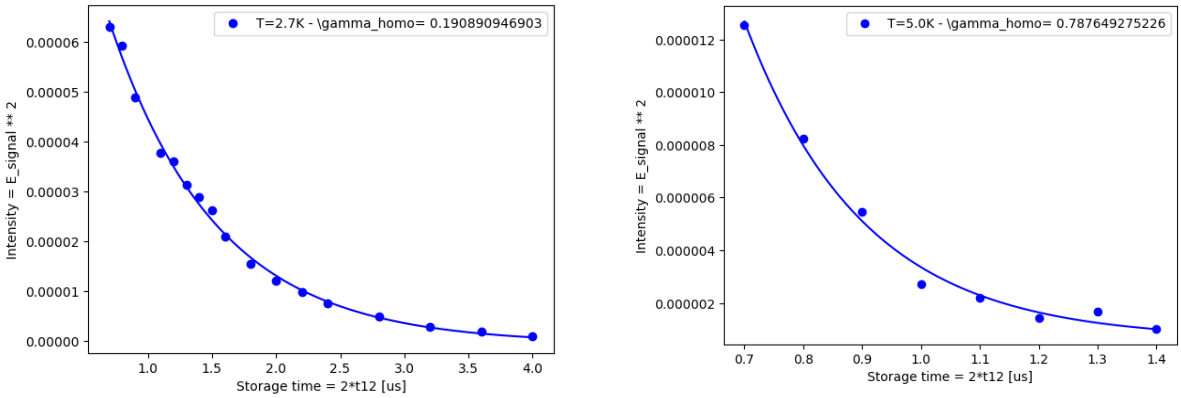

***Figure 4**: Intensity of two-pulse echo as a function of storage time for 200 ppm ceramics, for 2.7 K (left) and 5 K (right).*

The data is fitted using $I_{echo}(t_{12}) = I_0\, e^{-\frac{4t_{12}}{T_2}}$ from where T_2 is extracted and then γ_{homo} calculated. Finally, Fig 5 shows the plot of γ_{homo} vs temperature.

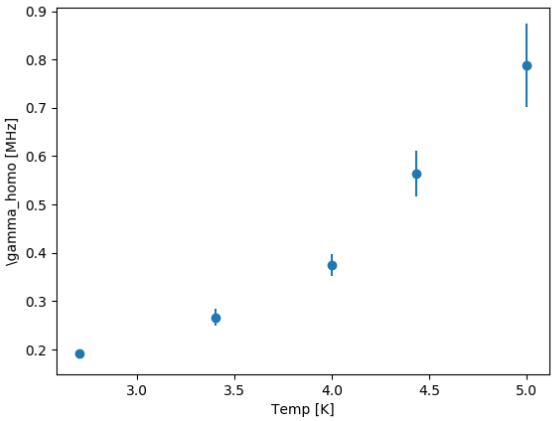

***Figure 5**: Homogeneous linewidth of Er^{3+}:Y_2O_3 ceramic with a concentration of 200 ppm, as a function of the cold finger temperature.*

We see that the homogeneous linewidth is as small as 200 kHz at 2.7 K. This value is promising for experiments aiming at single ion detection with a fiber micro-cavity. However, it is currently very challenging to reach this low temperature in the fiber cavity setup. Nevertheless, γ_{homo} remains below 1 MHz even for temperatures as high as 5 K. This value is encouraging, as it is still 3 orders of magnitude below the linewidth of the cavity, which is in the GHz regime, at a temperature of 5 K. Previous studies at CNRS-CP have shown that the values obtained in ceramics are usually a good indication of what can be achieved in nanocrystals.

These measurements were done for a relatively small magnetic field of around 20 Gauss. It is well known that optical T_2 in erbium is heavily dependent on magnetic field, so it will be interesting to study the magnetic field dependence for this sample for which an electromagnet has to be acquired. It is worth noting that a strong magnetic field dependence has been observed for the optical T_2 in Nd^{3+}: Y_2O_3 ceramics by ULUND (see D2.5). Since Nd^{3+} is also a paramagnetic rare-earth ion, we expect Er^{3+} to show similar behavior, i.e. optimal fields of a few 100s of mT. We have also tried to implement spectral hole burning but unfortunately, we could not measure it, probably as the magnetic field was too weak. We also note that the measurements were performed using a closed-cycle cold-finger cryostat. The thermal link between the ceramics and the cold finger might have not been optimum.

Characterization of single Er^{3+}:Y_2O_3 nano-particles

We have also performed spectroscopy measurements for single erbium doped nanoparticles at low temperature. The particles were spin-coated on a mirror and embedded into a high finesse fiber-based microcavity, as explained in detail in deliverable D2.7. We have been able to measure the inhomogeneous broadening and the optical lifetime of several nanoparticles. The particles were excited in resonance from the optical fiber using a pulsed laser at 1535 nm. The emitted fluorescence was then collected in the fiber as well, after the excitation laser was turned off, and directed towards a single photon detector. Fig. 6 (left) shows the inhomogeneous broadening of a nanoparticle of diameter 240 nm containing around 40'000 ions. We measure an inhomogeneous broadening of 10 GHz. This is slightly larger than the value measured in the ceramics and is attributed to the different synthesis methods between the ceramics and nanoparticles. In the latter case, crystals are obtained from a hydro-carbonate precursor and some -OH and -CO groups could remain in the particles even after high-temperature annealing. Measurements on smaller particles (diameter 170 nm) gave slightly larger values between 13 and 15 GHz. The T_1 lifetime measurement is shown in Fig. 6 (right) for the 240 nm particle. The measured T_1 is 16.5 ms. The T_1 is measured by setting the cavity on resonance after a variable time after the excitation, as explained in more details in D2.7.

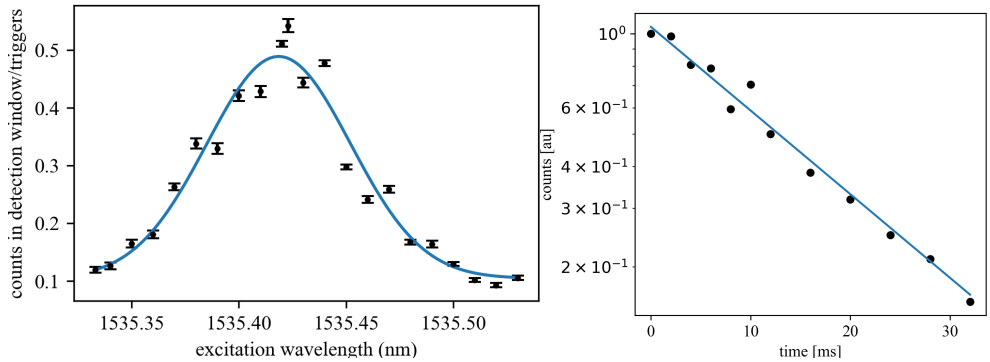

***Figure 6**: (left) the inhomogeneous broadening of a nanoparticle of diameter 240 nm containing 40'000 ions (right) T_1 lifetime measurement performed in the same nanocrystal.*

Optical and spin coherence in Pr^{3+}: Y_2O_3 nanostructures

In addition to the coherence properties of Er^{3+}: Y_2O_3 materials, we also investigated Pr^{3+}: Y_2O_3 ceramics and nanoparticles. Pr is a non-Kramers ion which displays long optical and spin coherence lifetimes in bulk crystals, and which has been extensively used for demonstrations of solid-state optical quantum memories [2-4]. In the context of the detection of single ions, Pr^{3+} ions may be an alternative to Eu ions or Er ions. While their optical and spin coherence lifetimes are shorter than in Eu, Pr ions present several advantages. In Y_2O_3, the Pr^{3+} $^1D_2(0)$ - $^3H_4(0)$ transition is expected to exhibit, at least, one order of magnitude larger oscillator strength than the Eu^{3+} $^7F_0$ -$^5D_0$ transition [5]. The optical population lifetime is around 150 µs, a factor of 10 shorter than in Eu and 100 shorter than Er. Higher emission branching compared to Eu ratio is equally expected from luminescence investigations carried out in other compounds [5]. However, very few previous studies exist on optical homogeneous lines in Pr^{3+}: Y_2O_3 [6] while hyperfine structures and spin homogeneous lines have never been reported.
To assess the potential of Pr for single ion detection experiments, we have carried out a complete high-resolution and coherent optical and nuclear spin spectroscopic investigation of $^{141}Pr^{3+}$: Y_2O_3 ceramics and nanoparticles. This work is described in full details in [7], we give here a summary of the main results. The samples have been fabricated by CNRS-CP in the same way as the Er doped samples described above, and the spectroscopy was performed in CNRS-CP premises, in collaboration with ICFO-QP.

Optical inhomogeneous and homogeneous linewidths

We have measured the optical homogeneous linewidth of Pr^{3+}: Y_2O_3 ceramics and nanoparticles, using two-pulse photon echoes. The echo decay curves are shown in Fig 7. Coherence lifetimes of 3 μs and 1 μs were extracted from exponentially decaying fits, corresponding to homogeneous lines $= (\pi T_2)^{-1}$ of 108 kHz and 315 kHz for 400 nm and 150 nm-diameter particles respectively. These values are narrower than those reported in some particular bulk Pr^{3+}: Y_2O_3 crystals [6] although they still remain far from the 1.1 kHz linewidth given by the optical T_1 limit. T_1 is found equal to 140 μs in the nanoparticles. In previous work, the dominant optical dephasing mechanism in Eu^{3+}: Y_2O_3 nanoparticles has been attributed to fluctuating electric fields associated to charged surface states [8]. The broader homogeneous line found here for the 150 nm-diameter particles (Fig. 7) is consistent with this hypothesis since surface to volume ratios increase as the particle size decreases. Nonetheless, it seems that the observed broadening is better explained by the decrease in crystalline grain size rather than particle size.

Crystalline domains decrease from 120 nm to 80 nm from 400-nm-diameter to 150-nm-diameter particles. Therefore, the electric field strength at the center of a crystallite is about 2.3 times larger in an 80-nm crystallite than a 120-nm one. This assumes that the field originates from electric charges located at the interface between crystallites. In contrast, if we take into account electric noise originated at the nanoparticles outer surface, 7 times larger electric field strength is expected in the 150-nm particles. This should lead to larger broadening than experimentally observed. In a similar way, the impact of the crystalline domain size over the particle size in the optical dephasing has been recently evidenced on Eu^{3+}: Y_2O_3 nanoparticles [9].

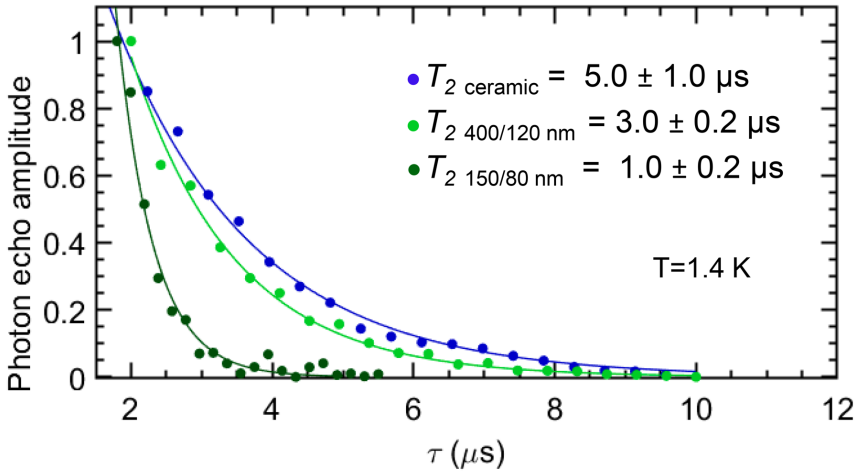

***Figure 7**: echo decay curves for different samples.*

Spin homogeneous linewidths

Spin homogenous linewidths have been measured on the nanoparticles using a two-pulse Raman spin echo technique. Fig. 8 shows the decay of the echo amplitude as function of the pulse delay for nanoparticles of 400 nm and 150 nm diameter. From the single exponential decays, T_2 times of 880 (40) μs and 640 (30) μs, respectively, can be inferred. Interestingly, these values are larger than the one obtained in bulk Pr^{3+}: Y_2SiO_5 crystals [10].

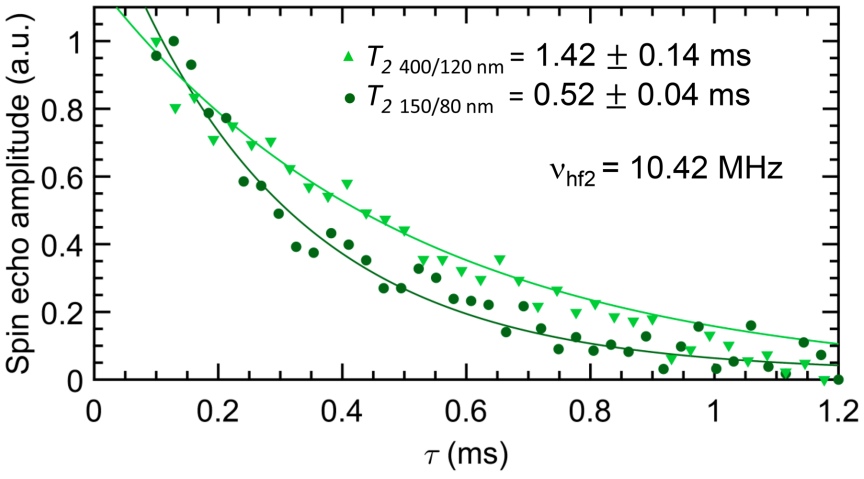

***Figure 8**: spin echo decay curves for different samples.*

Discussion

The relaxation and coherence properties here demonstrated for $^{141}Pr^{3+}$ in nanoscale Y_2O_3 appear very appealing for applications of this material in quantum devices. The results are summarized in Table I. Among them, the long spin dephasing times found in nanoparticles at zero external magnetic field is particularly promising. Unlike the optical transition, spin transitions are rather insensitive to electric perturbations given by their low nuclear Stark coefficient: four orders of magnitude lower than the optical one [11]. Thus, spin dephasing is here most likely due to magnetic interactions, as concluded for Eu^{3+}: Y_2O_3 nanoparticles [12] and in general for many bulk rare-earth doped crystals [13]. Still, in view of the present results, the magnetic sensitivity of Pr^{3+}in Y_2O_3 appears lower than in other crystalline hosts including Y_2SiO_5. This can be explained by the larger crystal field splitting in Y_2O_3 compared to other materials. This gives rise to lower second-order contributions and results in smaller hyperfine splittings and gyromagnetic ratios. Furthermore, we note that the spin coherence results presented here are obtained, not from bulk single crystals, but nanoparticles down to 150 nm. Hence, Pr^{3+}: Y_2O_3 is a highly performing material at the nanoscale.

	Ceramic	400/120 nm	150/80 nm
Optical			
Γ_{inh} (GHz)	9	27	
T_1 (μs)	140	140	
T_2 (μs)	4.5±0.5	3.0±0.3	1.0±0.1
$\Gamma_{h,opt}$ (kHz)	72±16	108±21	315±64
Spin			
T_1 (s)	5	7	
$\Gamma_{inh,5.99}$ (kHz)	29±2	42±9	
$\Gamma_{inh,10.42}$ (kHz)	29±2	48±6	
$T_{2,5.99}$ (μs)	730±50	680±40	640±40
$\Gamma_{h,5.99}$ (Hz)	440±60	470±50	500±50
$T_{2,10.42}$ (μs)	730±20	880±40	640±30
$\Gamma_{h,10.42}$ (Hz)	430±30	360±40	500±40

TABLE I. Summary of spectral and relaxation parameters determined for $^{141}Pr^{3+}$: Y_2O_3 ceramic and two sizes of nanoparticles. Spin T_2 values for the ceramic sample are here given for the sake of comparison.

Conclusions

We have measured spectroscopic properties such as coherence time, inhomogeneous broadening of the optical transition and population lifetime of the excited state of erbium doped ceramics and nanoparticles, fabricated by CNRS-CP. We first performed measurements at room temperature, where we found optical linewidth of 130 GHz for nanoparticles. At low temperature, we performed measurements on Er^{3+}: Y_2O_3 ceramics and found an inhomogeneous broadening of the optical transition of between 4 and 8 GHz, depending on the sample, and a lifetime of 9 ms. We also measured optical homogeneous linewidth as low as 200 kHz for a temperature of 2.7 K, and 800 kHz at 5 K. These values are promising for cavity-enhanced single ion detection, as they are more than 3 orders of

magnitude smaller than the fiber cavity linewidth operative at ICFO-QP. Homogeneous linewidth measurements on Er doped nanoparticles by photon echoes have not been so far successful. This could be due to too high temperature, as the loose powders tend to show low thermal conductivity. We also performed cavity-enhanced spectroscopic measurements of single erbium doped nanoparticles, showing larger inhomogeneous broadening that in the ceramics (10-15 GHz) and longer population lifetimes (16 ms).

We also report the spectroscopic characterization of a promising alternative material for nanoscale applications: Pr^{3+}:Y_2O_3. We have measured the optical and spin coherence and population lifetimes of nanoparticles. We determined optical homogeneous linewidths of the order of 100 kHz for nanoparticles of 400 nm diameter and 300 kHz for 150 nm particles. The values observed for the spin coherence are particularly promising, reaching up to 800 μs. This is longer than what is measured in bulk crystals of Pr^{3+}: Y_2SiO_5, which shows that the spin-coherence is not affected by using nanomaterials. This is especially important in view of realizing long-lived spin-photon interfaces.

Importantly, we note that so far, optical coherence lifetimes in nanoparticles do not appear fundamentally limited. Moreover, we have demonstrated that optical T_2 extension can be obtained by post-synthesis treatments. Further improvement should therefore be possible by increasing the particles crystalline quality and reducing defects.

References

[1] K. de Oliveira Lima, R. Rocha Gonçalves, D. Giaume, A. Ferrier, and P. Goldner, "Influence of defects on sub-Å optical linewidths in Eu^{3+}:Y_2O_3 particles," J. Lumin. 168, 276–282 (2015).

[2] M. Gündoğan, P. M. Ledingham, K. Kutluer, M. Mazzera, and H. de Riedmatten, "Solid State Spin-Wave Quantum Memory for Time-Bin Qubits," Phys. Rev. Lett. 114, 230501 (2015).

[3] K. Kutluer, E. Distante, B. Casabone, S. Duranti, M. Mazzera, and H. de Riedmatten, "Time Entanglement between a Photon and a Spin Wave in a Multimode Solid-State Quantum Memory," Phys. Rev. Lett. 123, 030501 (2019).

[4] N. Maring, P. Farrera, K. Kutluer, M. Mazzera, G. Heinze, and H. de Riedmatten, "Photonic quantum state transfer between a cold atomic gas and a crystal," Nature 551, 485–488 (2017).

[5] D. L. McAuslan, J. J. Longdell, and M. J. Sellars, "Strong-coupling cavity QED using rare-earth-metal-ion dopants in monolithic resonators: What you can do with a weak oscillator," Phys. Rev. A 80, 062307 (2009).

[6] T. Okuno and T. Suemoto, "Systematic control of spectral hole burning and homogeneous linewidth by disorder in Y2O3 : Pr3+ crystalline systems," Phys. Rev. B 59, 9078–9087 (1999).

[7] D. Serrano, C. Deshmukh, S. Liu, A. Tallaire, A. Ferrier, H. de Riedmatten, P. Goldner, "Coherent optical and spin spectroscopy of nanoscale Pr^{3+}:Y_2O_3", arXiv:1909.02260, accepted in Phys. Rev. B.

[8] J. G. Bartholomew, K. de Oliveira Lima, A. Ferrier, and P. Goldner, "Optical Line Width Broadening Mechanisms at the 10 kHz Level in Eu3+:Y2O3 Nanoparticles," Nano. Lett. 17, 778–787 (2017).

[9] S. Liu, D. Serrano, A. Fossati, A. Tallaire, A. Ferrier, and P. Goldner, "Controlled size reduction of rare earth doped nanoparticles for optical quantum technologies," RSC Adv. 8, 37098–37104 (2018).

[10] E. Fraval, M. J. Sellars, and J. J. Longdell, "Method of Extending Hyperfine Coherence Times in Pr3+:Y2SiO5," Phys. Rev. Lett. 92, 077601 (2004).

[11] R. M. Macfarlane, A. Arcangeli, A. Ferrier, and P. Goldner, "Optical Measurement of the Effect of Electric Fields on the Nuclear Spin Coherence of Rare-Earth Ions in Solids," Phys. Rev. Lett. 113, 157603 (2014).

[12] D. Serrano, J. Karlsson, A. Fossati, A. Ferrier, and P. Goldner, "All-optical control of long-lived nuclear spins in rare-earth doped nanoparticles," Nat. Commun. 9, 2127 (2018).

[13] P. Goldner, A. Ferrier, and O. Guillot-Noël, "Rare Earth-Doped Crystals for Quantum Information Processing," in Handbook on the Physics and Chemistry of Rare Earths, J.-C. G. Bünzli and V. K. Pecharsky, eds. (Elsevier, 2015), Vol. 46, pp. 1–78.